Journal of the Serbian Chemical Society
JSCS-info@shd.org.rs • www.shd.org.rs/JSCS
J. Serb. Chem. Soc. *84* (12) 1415–1426 (2019)
JSCS–5274
UDC 546.56+546.137–145.2:544.654.2:544.653.1
Original scientific paper

Tuning the copper cluster's size on HOPG by electrodeposition from perchlorate aqueous solutions. An AFM study

DIANA ELIZABETH GARCIA-RODRIGUEZ[1], CLARA HILDA RIOS REYES[2] and LUIS HUMBERTO MENDOZA HUIZAR[3]*

[1]*Comunidad Educativa Entorno. Eugenio Garza Sada No. 72. Los Pocitos. Aguascalientes, México,* [2]*Artes. San Felipe 215. Providence. Mineral de la Reforma Hidalgo, Hgo. México and* [3]*Universidad Autónoma del Estado de Hidalgo. Academic Area of Chemistry. Carretera Pachuca-Tulancingo Km. 4.5 Mineral de la Reforma, Hgo, México*

(Received 23 January, revised 2 April, accepted 29 May 2019)

Abstract: In this work, we report the electrochemical synthesis of nanometric copper clusters smaller than 3 nm of height and 14.3 nm of diameter from perchlorate solutions. From the number of copper clusters counted directly from the AFM (Atomic force microscopy) images, it was possible to derive an equation, which is able to predict the number of clusters formed in function on the applied potential. Also, qualitative AFM images were simulated employing a spreadsheet and the freeware ImageJ, the results obtained show concordance with the experimental AFM images.

Keywords: copper; nanocluster; instantaneous nucleation; potentiostatic; AFM.

INTRODUCTION

Copper nanoparticles (CuN) have been widely used as cooling fluids for electronic systems,[1] conductive inks,[2] biosensors,[3] electrochemical sensors,[4] antimicrobial agents,[5] among others. Also, CuN exhibit great catalytic activities, and nonlinear optical properties, which could result in many applications in optical devices and nonlinear optical materials, such as optical switches or photochromic glasses.[6,7] Moreover, recently, it was reported that CuN are able to convert CO_2 in methanol, which represents an important advance in diminishing some environmental issues in big cities.[8] Thus, it is not so strange that many researchers have been developing new methods to synthesize CuN. Currently the main methods to synthesize them include chemical reduction,[9–12] thermal decomposition,[13] polyol,[14,15] laser ablation,[16] in situ chemical synthetic route,[17] low energy cluster beam deposition technique[18] and electrodeposition.[4,19–22] Specifically, electrodeposition is commonly used to synthesize nanoparticles

* Corresponding author. E-mail: hhuizar@uaeh.edu.mx
https://doi.org/10.2298/JSC190123054G

because it is a relatively simple and low cost procedure in comparison with other techniques.[22] However, it is important to highlight that the physical and chemical properties exhibited by CuN are highly dependent on their size and morphology by which, one of the main difficulty during their synthesis is tailoring and fine--tuning the cluster's size and the properties of these for a given application.[23] In the case of the electrodeposition process, there are two main approaches to control the size of metallic nanoparticles. The first one is to vary the experimental conditions associated with the plating bath, while the second one is to modify the electrode surface roughness.[22] In the first approach, several parameters including the nature of additives, concentration of nanoparticle precursors, temperature, deposition potential, and the pH value of the plating bath, can be varied to ensure shape and size control of the nanoparticles,[24–28] while in the second approach, the electrode surface roughness is modified using either physical methods[29] or depositing conducting films[27]. Employing the first approach, Huang *et al*. were able to synthesize CuN of 51 nm on HOPG applying a potential step to nucleate copper particles, followed of a strip peak potential to strip smaller metal nuclei partly, at last, a growth potential.[21] Also, CuN have been synthesized modifying the composition of the plating bath by pectin scaffold[4] or using sulfate solutions.[30] On the other hand, the roughness surface may be modified depositing a polypyrrole conducting film on a substrate, and the size distribution of the CuN is highly dependent on the thickness of the polypyrrole film, due to the increased surface roughness and the decreased uniformity of the surface potential.[27] Thus, employing any of the two procedures above mentioned it has been possible to synthesize CuN with different sizes and distributions. From these results, it is clear that the modulation of the cluster's size depends on an extensive number of parameters, which have to be modified to get nanoparticles with a defined size and specific properties. Therefore, the development of simple methodologies is desirable to modulate the CuN's size electrodeposited on different substrates. Up to the best of our knowledge, the influence of the applied potential on the electrode surface to control the size of the copper nanoclusters from a plating bath based on perchlorate ions has not been reported in the literature. This kind of electrolyte shows advantages because ClO_4^- are weakly adsorbed on the electrode surface, which allows to study the nucleation process without a strong interference of anions adsorbed on the substrate.[19] Thus, in the present work we employed the potentiostatic technique to synthesize the copper clusters with different size, maintaining constant the composition of the plating bath and modifying exclusively the applied potential on the electrode surface. We carry out the morphological characterization of the CuN employing atomic force microscopy at different applied overpotentials. Also, we performed the prediction of qualitative AFM images of the CuN synthesized employing a spreadsheet and the freeware ImageJ.[31]

EXPERIMENTAL

The copper electrodeposition onto HOPG electrode was carried out from a plating bath containing 0.01 M $Cu(ClO_4)_2$ + 0.02 M $NaClO_4$ at pH 5. All plating baths were prepared using analytic grade reagents and ultra pure water (Millipore-Q system) and they were deoxygenated by bubbling N_2 for 15 min before each experiment. For these experiments, freshly cleaved HOPG surfaces were employed in each experiment. In all cases a graphite bar was used as counter electrode, while an Ag/AgCl electrode (in saturated KCl), with a Luggin capillary was used as reference electrode. All potentials are expressed on Ag/AgCl scale. All experiments were carried out at 25ºC in unstirred solutions. An Epsilon potentiostat with the BASi-EpsilonEC software was employed to control the parameters involved during the electrochemical experiments. Cyclic voltammetry was carried out in the 0.600 V to –0.800 V potential range. The characterization of CuN was performed with an atomic force microscopy (AFM) a JEOL JSPM 4210 microscope in the lift mode.

RESULTS AND DISCUSSION

A cyclic voltammogram was obtained from the system 0.01 M $Cu(ClO_4)_2$ + 0.02 M $NaClO_4$ at pH 5, see Fig. 1. This voltammogram is similar to those reported previously by our research group.[19] Note that at the direct scan, the copper reduction process starts at 0.020 V approximately. Copper reduction process involves two-steps, the first one is a slow step, related to the reduction of Cu^{2+} to Cu^{1+} (peak A), while the second one is a fast step related to Cu^{1+} to Cu (peak B).[32] The peak A at –0.050 V has been associated with the slow step, while peak B at –0.2 V, is related to the fast step. Thus, from this voltammogram it can be seen that metallic copper can be electrodeposited at lower potentials than –0.050 V.

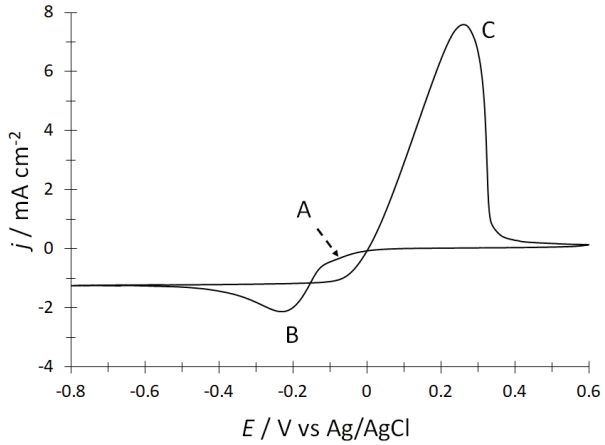

Fig. 1. A typical cyclic voltammetric curve obtained onto a HOPG electrode from an aqueous solution containing 0.01M $Cu(ClO_4)_2$ + 0.02M $NaClO_4$ (pH 5.0). The potential scan rate was started at 0.600 V toward the negative direction with a potential scan rate of 20 mV s^{-1}.

It is possible to synthesize metallic clusters employing the chronoamperemetric technique, however, it is necessary to know the potential value, and the

duration of the potential pulse applied on the electrode surface. Here, it is important to mention that from *j vs. t* plots is possible to infer the experimental potential values where is possible to form disperse clusters. In this work, the transients were obtained by applying an initial potential of 0.600 V on the electrode surface. After the application of this initial potential, a step of negative potential was varied on the electrode surface in the range -0.075 to -0.175 V. In this sense, the formation of a current density maximum in a transient may serve to identify the regions in where it is possible synthesize, either disperse or overlapped clusters. Thus, before this maximum it is possible to synthesize clusters because the nucleation process is separated from the overlapping process.[35] In Fig. 2, it is reported a chronoamperogram obtained from the HOPG/0.01M $Cu(ClO_4)_2$ + 0.02 M $NaClO_4$ (pH 5) system at –0.175 V *vs.* Ag/AgCl for 30 s. Note that this potential value corresponds to the extreme of the potential range analyzed in the present work. This transient is similar to those reported previously for the copper electrodeposition of copper onto HOPG electrodes by our research group.[19]

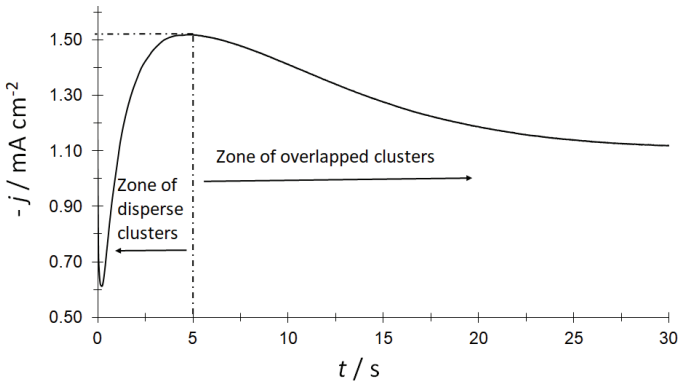

Fig. 2. Chronoamperogram obtained with the potentiostatic technique from the HOPG/0.01 M $Cu(ClO_4)_2$ + 0.02 M $NaClO_4$ (pH 5) system at –0.175 V *vs.* Ag/AgCl.

Moreover, in the transients reported in the previous work, is clear that the transients obtained at more negative potentials than –0.175 V, show diffusion limitations which become significant and may alter the getting of disperse clusters. Thus, we selected the potential range in the present work as –0.075 to –0.175 V to carry out the present study, because in this range it is possible to adequately control the influence of the applied potential involved in the formation of copper clusters. Also, from Fig. 2 it is possible to note that the current density maximum is obtained at 5 s, therefore, at this applied potential value the formation of copper clusters should be obtained at $t \leq 5$ s, and at $t > 5$ s is expected the overlapping of the copper clusters.

Thus, in the present work, in all cases, the potential pulse was finalized at 5 s to avoid the overlapping of nuclei (clusters) on the electrode surface, see Fig. 3.

The transients obtained at the potentials values reported in Fig. 3 but at $t > 30$ s, have already been reported previously by our research group.[19] In the transients reported in Fig. 3, note that at shorter times than 0.5 s, there is a falling current transient, which may be associated with a process where the adsorption and the step Cu^{2+} to Cu^{1+} occurs simultaneously at the HOPG electrode surface.[33,34] Also, note that after this falling current, in each case, the *j vs. t* plot increase the density current value without reaches a maximum, this fact ensures the formation of disperse copper clusters on the HOPG surface.

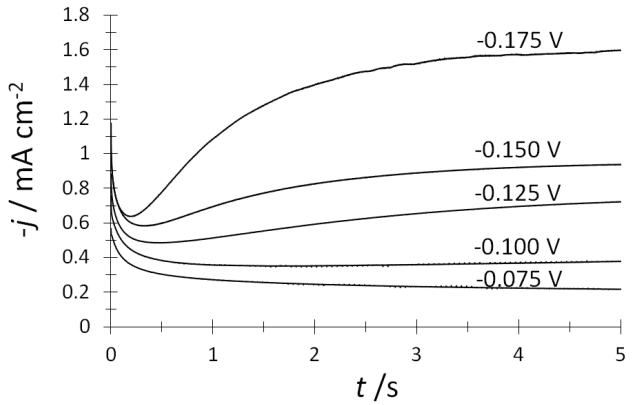

Fig. 3. A set of current transients obtained from aqueous solution 0.01 M $Cu(ClO_4)_2$ + 0.02 M $NaClO_4$ (pH 5) onto a HOPG by means of the potential step technique for different potential step values indicated in the figure. In all the cases, the initial potential was 0.600 V.

The general shape of the transients reported in Fig. 3 is very similar to the reported for a three dimensional nucleation process with a diffusion control (3D-c).[36,37] A classification of the nucleation as instantaneous or progressive from transients showed in Fig. 3 is possible by following the criteria established by Sharifker *et al.* where the experimental transients in a non-dimensional form by plotting j^2/j_m^2 *vs.* t/t_m are compared with those theoretically generated from Eqs. (1) and (2) for instantaneous and progressive nucleation, respectively:[36]

$$\frac{j^2}{j_m^2} = 1.9254\left(\frac{t}{t_m}\right)^{-1}\left\{1-\exp\left[-1.2564\left(\frac{t}{t_m}\right)\right]\right\}^2 \quad (1)$$

$$\frac{j^2}{j_m^2} = 1.2254\left(\frac{t}{t_m}\right)^{-1}\left\{1-\exp\left[-2.3367\left(\frac{t}{t_m}\right)^2\right]\right\}^2 \quad (2)$$

where j_m is the current density on the maximum reached at the time t_m. However, it is important to mention that these equations are valid only at the initial stages

of the electrocrystallization process, when the nuclei are sufficiently small and growth to independently from each other.[38]

Fig. 4 shows a comparison of the theoretical dimensionless transients, generated by Eqs. (1) and (2) with the experimental dimensionless current transients reported in Fig. 3. This analysis was carried out for the transients obtained at –0.175, –0.150 and –0.125 V during a pulse potential of 5 s, to ensure the formation of disperse copper clusters on the HOPG surface. Note that the nucleation process may be classified as instantaneous. In an instantaneous nucleation the saturation number density of nuclei is achieved immediately after applying the potential step, by which is possible to control the number of cluster formed on the electrode. Moreover, in an instantaneous nucleation is expected that all nuclei have similar sizes.

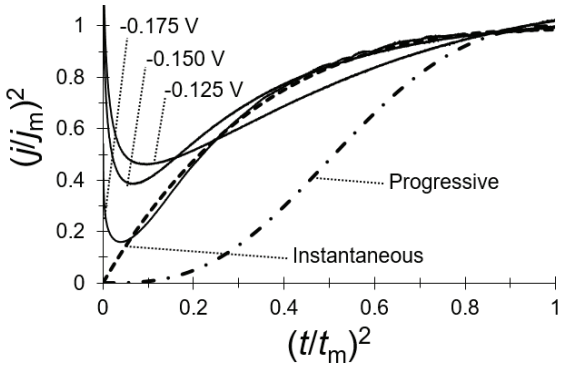

Fig. 4. Comparison of experimental transients obtained at different potential values normalized through the coordinates of its respective local maximum (t_m, j_m), with the theoretical non-dimensional curves corresponding to 3D instantaneous nucleation (Eq. (1)) and 3D progressive nucleation (Eq. (2)).

In order to verify the formation of CuN on the HOPG surface through the potentiostatic technique, we analyzed the copper deposits electrochemically synthesized when the potentials applied on the electrode surface were –0.075, –0.100, –0.125, –0.150 and –0.175 V. For the case of the transients obtained at –0.075 V (see Fig S-1a of the Supplementary material to this paper) and –0.100 V (see Fig. 5); it is possible to observe the formation of disperse copper clusters on the HOPG surface. The AFM images reported in these figures were visualized with the software WSxM.[39] Note that when the applied potential was –0.125 V (Fig. S-1b) the number of copper clusters is major in comparison with the nuclei population observed at –0.075 and –0.100 V. A similar behaviour is observed at the –0.150 (Fig. S-1c) and –0.175 V (Fig. S-1d) applied potentials. Thus, at lower potentials the population of nuclei on the electrode surface is bigger. Moreover, note that in all cases the copper clusters synthesized are homogeneous and they

are disperse on the electrode surface, which agrees with the concluded from the non-dimensional plots, see Fig. 4. Last results suggest that it is possible to control the population of copper clusters synthesized on the HOPG surface with a simple change on the applied potential on the electrode surface.

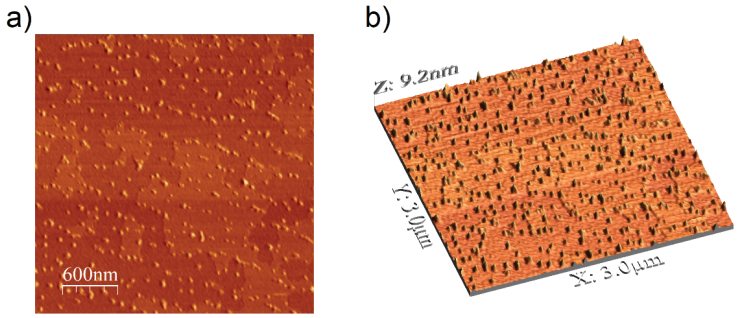

Fig. 5. AFM image of the copper clusters electrodeposited on HOPG electrode at –0.100 V, from a plating bath containing 0.01 M $Cu(ClO_4)_2$ + 0.02 M $NaClO_4$ at pH 5; a) 2D; b) 3D.

In order to determine the average cluster's size of the copper clusters obtained at each potential; we plotted the distribution of cluster's size as function of their height employing the WSxM software.[39] Also, the roughness of the HOPG substrate in an area of 3.0×3.0 μm^2, covered with copper clusters, was measured; resulting 0.35, 0.39, 0.51, 0.83 and 0.89 nm for the deposits obtained at -0.075, -0.100, –0.125, –0.150 and –0.175 V, respectively. Note that the roughness becomes higher as the number of nuclei or clusters increases due to the changes on the surface morphology. The average cluster's size at each case was evaluated considering a Gaussian distribution. In Fig. 6, it is reported the histo-

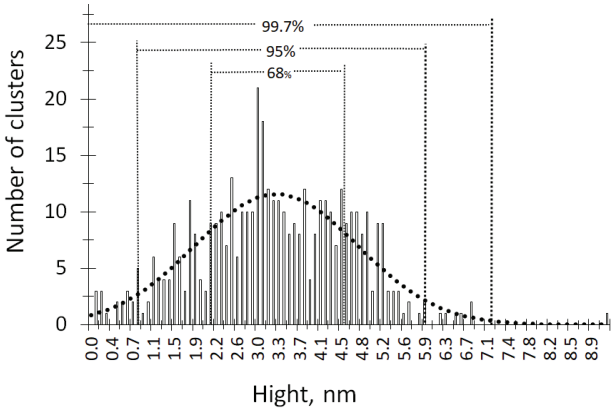

Fig. 6. Histogram of the height distribution of copper clusters deposited at –0.100 V potential value in an area of 3.0×3.0 μm^2, and its corresponding Gaussian distribution. Also, height cluster distribution is depicted according to the three-sigma rule.

gram for the number of copper clusters deposited at –0.100 V in an area of 3.0×3.0 μm^2; and its corresponding Gaussian distribution, for this potential value, the average cluster's size is 3.3 nm. A similar analysis was carried out for the other cases, and the average cluster's size is 3.6, 3.1, 2.4, and 2.3 nm for -0.075, –0.125, –0.150 and –0.175 V, respectively. Also, note in Fig. 6 that, according to the three-sigma rule, 68 % of the cluster's size is in the range of 2.06–4.63 nm, 95 % in the range 0.8–5.91 nm and 99.7 % in the range 0–7.20 nm. Thus, copper clusters bigger than 7.2 nm are few and their influence is negligible in the Gaussian distribution.

Considering the above mentioned we selected different zones of the AFM images reported in Figs. 5 and S-1 (see Supplementary material), where the copper cluster's size is into the 95 % of the Gaussian distribution, to avoid the influence of the clusters, which are not significant in the analysis. In Fig. S-2 of the Supplementary material, these zones can be seen, on each image reported in this figure; we carried out a similar analysis to that shown in Fig. 6. The results obtained indicates that the average cluster's size for –0.075, –0.100, –0.125, –0.150 and –0.175 V applied potentials values are 2.84, 2.77, 2.69, 2.65, and 1.98 nm, respectively. The *RMS* (root mean square) associated with these electrodeposits were 0.35, 0.31, 0.27, 0.35 and 0.45 nm. Also, to determine the diameter of the copper clusters we used the OTSU thresholding method as implemented in the software Gwyddion.[40] Thus, for –0.075, –0.100, –0.125, –0.150 and –0.175 V the average diameters are 14.3, 13.71, 11.41, 11.05 and 11.02 nm, respectively. These results are indicating that the cluster's size increases as the applied potential is augmented.

These results suggest that small copper clusters may be obtained when lower potential values are applied on the electrode surface, while bigger clusters were obtained at more positive potentials than –0.075 V. From Fig. S-2, the number of clusters obtained for –0.075, –0.100, –0.125, –0.150, and –0.175 V were 62, 84, 135, 167, and 248 per μm^2, respectively. It is clear that the population of nuclei is increased when the applied potential is more negative than –0.075 V. Also, observe that this increment follows an exponential tendency with the applied potential, see Fig. 7, which may be represented by the following equation:

$$N = 21.956e^{-0.0138E} \quad (3)$$

where N is the number of nuclei per μm^2, and E is the applied potential in mV.

Also, in this work we propose to simulate the qualitative AFM images of the copper clusters synthesized, through the number of nuclei and their respective xyz coordinates. Thus, it is possible to consider that all nuclei should have similar heigths because under our conditions the copper electrodeposition is instantaneous, see Figs. 5, S-1 and S-2. In order to perform the simulation of the AFM images, the number of nuclei at each potential were determined employing the Eq.

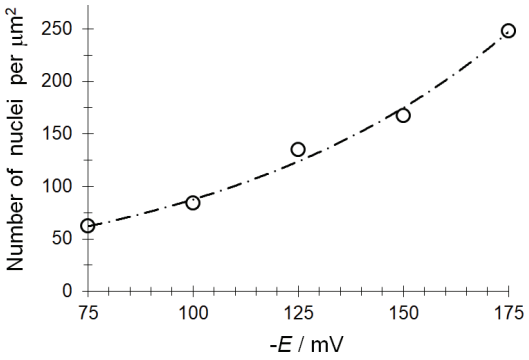

Fig. 7. Copper cluster's population in function of the applied potential derived from AFM images reported in Fig. S-2.

(3), and their respective xy coordinates were determined through the "random function" implemented in any spreadsheet, such as Excel™, multiplied by the long and wide of the modelled surface. For example the "*x*" coordinate is obtained as ("random function")×(wide), while the "*y*" coordinate is calculated as ("random function")×long, where "wide" and "long" correspond to the surface's dimensions. This approximation is valid because at the initial stages of the electrodeposition process the nuclei formation on the electrode surface follows a random distribution.[41] This procedure is repeated as many times as nuclei have been formed or predicted by Eq. (3) at a specific potential value. Once the *xy* coordinates of each nuclei are obtained they are plotted in a bidimensional arrengment, then this figure is visualized employing the freeware ImageJ,[31] and the plugin "Interactive 3D surface plot" as implemented in this software. Fig. 8 shows the simulation and distribution of nuclei on HOPG according to procedure above mentioned, on an area of 1 µm^2 (wide = 1 µm and long = 1 µm) for the experimental applied potential value of –0.075 V, the simulation for the other applied potentials are reported in Fig. S-3. Also, a theoretical additional applied potential value (–0.200 V) was analyzed employing the methodology above mentioned.

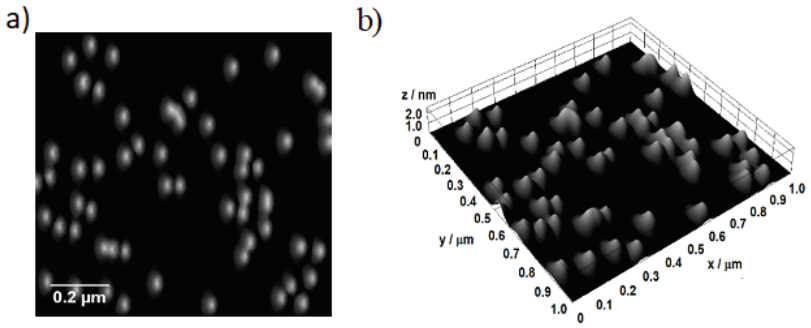

Fig. 8. Simulation of the distribution of the copper cluster nuclei per µm^2, according to Eq. (3) at the potential values of –0.075 V considering a random distribution of the nuclei on the HOPG surface; a) 2D; b) 3D.

Note that, according to this simulation, the formation of disperse clusters may be synthesized at higher potential than –0.175 V. From these simulations note that the agglomeration of nuclei is major at –0.175 and –0.200 V, which suggests that the synthesis of disperse copper clusters with nanometric dimensions may be carried out at higher potentials than –0.175 V. These results show a similar tendency to that observed from the experimental AFM study, see Fig. S-2, suggesting that this methodogy may be employed to simulate the population and distribution of CuN on the HOPG surface at different applied potential values.

CONCLUSION

In this work, we employed the potentiostatic technique to synthesize nanometric copper clusters from a plating bath based on perchlorate solutions on a HOPG electrode. Our results indicate that it is possible to synthesize copper clusters smaller than 3 nm of height and 14.3 nm of diameter from perchlorate solutions, modifying exclusively the applied potential on the electrode surface. From the AFM study, it was observed that the population of copper clusters is increased when the applied potential is more negative than –0.075 V, however higher clusters are obtained at more positive potentials.

SUPPLEMENTARY MATERIAL

Additional data are available electronically from http://www.shd.org.rs/JSCS/, or from the corresponding author on request.

Acknowledgements. LHMH gratefully acknowledges financial support from CONACYT (project CB2015-257823) and to the Universidad Autónoma del Estado de Hidalgo. Guanajuato National Laboratory (CONACyT 123732) is acknowledged for supercomputing resources. LHMH acknowledges to the SNI for the distinction of their membership and the stipend received.

ИЗВОД

ПОДЕШАВАЊЕ ВЕЛИЧИНЕ КЛАСТЕРА БАКРА ЕЛЕКТРОХЕМИЈСКИМ ТАЛОЖЕЊЕМ НА ВИСОКО ОРИЈЕНТИСАНОМ ПИРОЛИТИЧКОМ ГРАФИТУ. ИСПТИВАЊЕ МИКРОСКОПИЈОМ АТОМСКИХ СИЛА

DIANA ELIZABETH GARCIA-RODRIGUEZ[1], CLARA HILDA RIOS REYES[2] и LUIS HUMBERTO MENDOZA HUIZAR[3]

[1]Comunidad Educativa Entorno. Eugenio Garza Sada No. 72. Los Pocitos. Aguascalientes, México, [2]Artes. San Felipe 215. Providence. Mineral de la Reforma Hidalgo, Hgo. México u [3]Universidad Autónoma del Estado de Hidalgo. Academic Area of Chemistry. Carretera Pachuca-Tulancingo Km. 4.5 Mineral de la Reforma, Hgo, México

У раду је приказана синтеза нанометарских кластера бакра висине испод 3 nm и пречника мањег од 14,3 nm електрохемијским таложењем из перхлоратног раствора. На основу броја кластера бакра одређеног микроскопијом атомских сила (AFM) изведена је једначина која предвиђа број формираних кластера у зависности од примењеног потенцијала таложења. Такође, извршена је квалитативна симулација AFM слика коришћењем слободно доступног програма ImageJ и показано је да су оне у сагласности са експерименталним AFM сликама.

(Примљено 23. јануара, ревидирано 2. априла, прихваћено 29. маја 2019)

REFERENCES

1. H.-S. Kim, Sanjay, R. Dhage, D.-E. Shim, H Thomas Hahn, *Appl. Phys., A* **97** (2009) 791–798 (http://dx.doi.org/10.1007/s00339-009-5360-6)
2. T. Yonezawa, H. Tsukamoto, M. T. Nguyen, *Adv. Powder Technol.* **28** (2017) 1966 (http://dx.doi.org/10.1016/j.apt.2017.05.006)
3. H. Heli, M. Hajjizadeh, A. Jabbari, A. A. Moosavi-Movahedi, *Biosens. Bioelectron.* **24** (2009) 2328 (http://dx.doi.org/10.1016/J.BIOS.2008.10.036)
4. V. Mani, R. Devasenathipathy, S.-M. Chen, S.-F. Wang, P. Devi, Y. Tai, *Electrochim. Acta* **176** (2015) 804 (http://dx.doi.org/10.1016/J.ELECTACTA.2015.07.098)
5. M. El Zowalaty, N. A. Ibrahim, M. Salama, K. Shameli, M. Usman, N. Zainuddin, *Int. J. Nanomedicine* **8** (2013) 4467 (http://dx.doi.org/10.2147/IJN.S50837)
6. O. Mondal, A. Datta, D. Chakravorty, M. Pal, *MRS Commun.* **3** (2013) 91 (http://dx.doi.org/10.1557/mrc.2013.13)
7. T. M. D. Dang, T. T. T. Le, E. Fribourg-Blanc, M. C. Dang, *Adv. Nat. Sci. Nanosci. Nanotechnol.* **2** (2011) 1 (http://dx.doi.org/10.1088/2043-6262/2/1/015009)
8. C. Liu, B. Yang, E. Tyo, S. Seifert, J. DeBartolo, B. von Issendorff, P. Zapol, S. Vajda, L. A. Curtiss, *J. Am. Chem. Soc.* **137** (2015) 8676 (http://dx.doi.org/10.1021/jacs.5b03668)
9. C. Wu, B. P. Mosher, T. Zeng, *J. Nanoparticle Res.* **8** (2006) 965 (http://dx.doi.org/10.1007/s11051-005-9065-2)
10. H.-X. Zhang, U. Siegert, R. Liu, W.-B. Cai, *Nanoscale Res. Lett.* **4** (2009) 705 (http://dx.doi.org/10.1007/s11671-009-9301-2)
11. X. Cheng, X. Zhang, H. Yin, A. Wang, Y. Xu, *Appl. Surf. Sci.* **253** (2006) 2727 (http://dx.doi.org/10.1016/j.apsusc.2006.05.125)
12. W. Yu, H. Xie, L. Chen, Y. Li, C. Zhang, *Nanoscale Res. Lett.* **4** (2009) 465 (http://dx.doi.org/10.1007/s11671-009-9264-3)
13. M. Salavati-Niasari, F. Davar, *Mater. Lett.* **63** (2009) 441 (http://dx.doi.org/10.1016/J.MATLET.2008.11.023)
14. K. Woo, D. Kim, J. S. Kim, S. Lim, J. Moon, *Langmuir* **25** (2009) 429 (http://dx.doi.org/10.1021/la802182y)
15. B. K. Park, D. Kim, S. Jeong, J. Moon, J. S. Kim, *Thin Solid Films* **515** (2007) 7706 (http://dx.doi.org/10.1016/J.TSF.2006.11.142)
16. R. M. Tilaki, A. Iraji zad, S. M. Mahdavi, *Appl. Phys. A* **88** (2007) 415 (http://dx.doi.org/10.1007/s00339-007-4000-2)
17. K. Mallick, M. J. Witcomb, M. S. Scurrell, *Eur. Polym. J.* **42** (2006) 670 (http://dx.doi.org/10.1016/J.EURPOLYMJ.2005.09.020).
18. S. Mondal, S. R. Bhattacharyya, *AIP Conf. Proc.* **1447** (2012) 737 (http://dx.doi.org/10.1063/1.4710214)
19. D. E. García-Rodríguez, C. H. Mendoza-Huizar, Luis Humberto, Rios-Reyes, M. A. Alatorre-Ordaz, Química, *Quim. Nov.* **35** (2012) 699
20. A. Han, Y. Yang, Q. Zhang, Q. Tu, G. Fang, J. Liu, S. Wang, R. Li, *J. Electroanal. Chem.* **795** (2017) 116 (http://dx.doi.org/10.1016/j.jelechem.2017.04.058)
21. L. Huang, E. S. Lee, K. B. Kim, *Colloids Surfaces A Physicochem. Eng. Asp.* **262** (2005) 125 (http://dx.doi.org/10.1016/j.colsurfa.2005.03.023)
22. C. J. Yang, F. H. Lu, *Langmuir* **29** (2013) 16025 (http://dx.doi.org/10.1021/la403719c)
23. Y. Xia, Y. Xiong, B. Lim, S. E. Skrabalak, *Angew. Chemie Int. Ed.* **48** (2009) 60 (http://dx.doi.org/10.1002/anie.200802248)

24. I. Haas, S. Shanmugam, A. Gedanken, *J. Phys. Chem., B* **110** (2006) 16947 (http://dx.doi.org/10.1021/JP064216K)
25. M. J. Siegfried, K.-S. Choi, *Adv. Mater.* **16** (2004) 1743 (http://dx.doi.org/10.1002/adma.200400177)
26. A. Radi, D. Pradhan, Y. Sohn, K. T. Leung, *ACS Nano* **4** (2010) 1553 (http://dx.doi.org/10.1021/nn100023h)
27. X. J. Zhou, A. J. Harmer, N. F. Heinig, K. T. Leung, *Langmuir* **20** (2004) 5109 (http://dx.doi.org/10.1021/LA0497301)
28. R. Bakthavatsalam, S. Ghosh, R. K. Biswas, A. Saxena, A. Raja, M. O. Thotiyl, S. Wadhai, A. G. Banpurkar, J. Kundu, *RSC Adv.* **6** (2016) 8416 (http://dx.doi.org/10.1039/C5RA22683J)
29. X.-J. Huang, O. Yarimaga, J.-H. Kim, Y.-K. Choi, *J. Mater. Chem.* **19** (2009) 478 (http://dx.doi.org/10.1039/B816835K)
30. M. Raja, J. Subha, F. B. Ali, S. H. Ryu, *Mater. Manuf. Process.* **23** (2008) 782 (http://dx.doi.org/10.1080/10426910802382080)
31. C. A. Schneider, W. S. Rasband, K. W. Eliceiri, *Nat. Methods* **9** (2012) 671 (http://dx.doi.org/10.1038/nmeth.2089)
32. E. Mattsson, J. O. Bockris, *Trans. Faraday Soc.* **55** (1959) 1586 (http://dx.doi.org/10.1039/tf9595501586)
33. A. Milchev, T. Zapryanova, *Electrochim. Acta* **51** (2006) 4916 (http://dx.doi.org/10.1016/J.ELECTACTA.2006.01.030)
34. A. Milchev, T. Zapryanova, *Electrochim. Acta* **51** (2006) 2926 (http://dx.doi.org/10.1016/J.ELECTACTA.2005.08.045)
35. M. Rivera, C. H. Rios-Reyes, L. H. Mendoza-Huizar, *J. Magn. Magn. Mater.* **323** (2011) 997 (http://dx.doi.org/10.1016/J.JMMM.2010.11.088)
36. B. Scharifker, G. Hills, *Electrochim. Acta* **28** (1983) 879 (http://dx.doi.org/10.1016/0013-4686(83)85163-9)
37. B. R. Scharifker, J. Mostany, *J. Electroanal. Chem.* **177** (1984) 13 (https://doi.org/10.1016/0022-0728(84)80207-7)
38. B. R. Scharifker, J. Mostany, , in *Encycl. Electrochem*., M. Bard, A. J. Stratmann (Ed.), Wiley-VCH, Weinheim, 2007, pp. 512–539 (http://dx.doi.org/10.1002/9783527610426.bard020503)
39. I. Horcas, R. Fernández, *Rev. Sci. Instrument.* **78** (2007) 013705 (https://doi.org/10.1063/1.2432410)
40. D. Nečas, P. Klapetek, Cent. Eur. J. Phys. 10 (2012) 181 (https://doi.org/10.2478/s11534-011-0096-2)
41. M. Tomellini, M. Fanfoni, *Phys. Rev., B* **55** (1997) 14071 (http://dx.doi.org/10.1103/PhysRevB.55.14071).